

Potential-driven constructing interface and tensile strain of derived-Cu catalyst for boosting CO₂ electrocatalytic reduction

Fangfang Chang¹, Zihan Lin¹, Yongpeng Liu¹, Qing Zhang¹, Xiaolei Wang², and Zhengyu Bai^{1*}

¹Collaborative Innovation Center of Henan Province for Green Manufacturing of Fine Chemicals, Key Laboratory of Green Chemical Media and Reactions, Ministry of Education, School of Chemistry and Chemical Engineering, Henan Normal University, Xinxiang, Henan 453007, China. Email: baizhengyu@htu.edu.cn

²Department of Chemical and Materials Engineering, University of Alberta, Edmonton, Alberta T6G 1H9, Canada

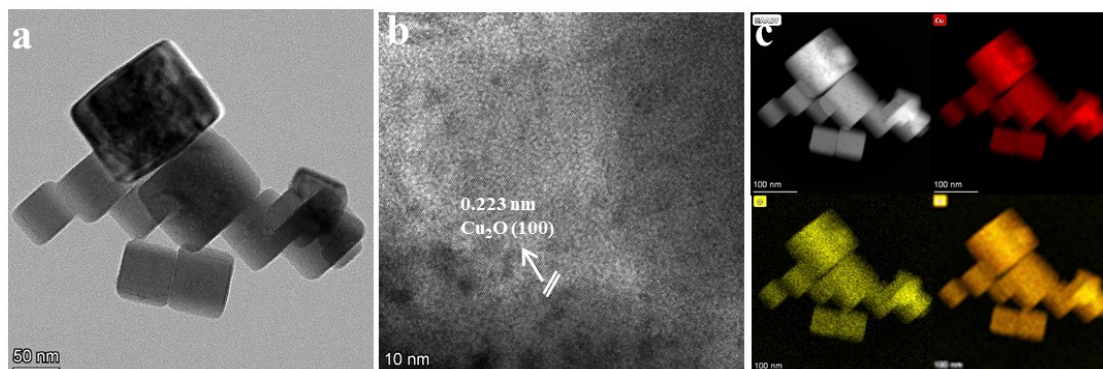


Fig. S1. (a) TEM, (b) HR-TEM, and (c) EDS-elemental mapping images of Cu₂O NCs.

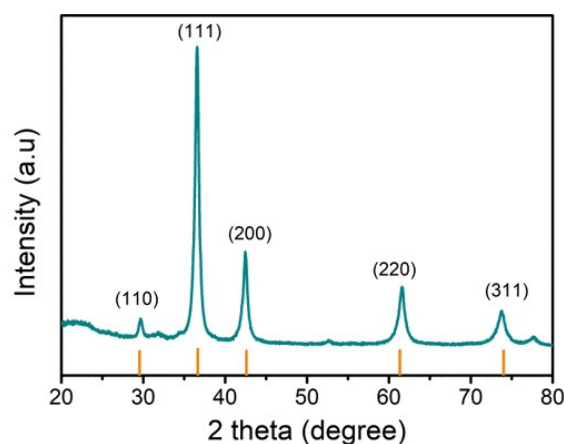


Fig. S2. XRD pattern of the Cu₂O NCs.

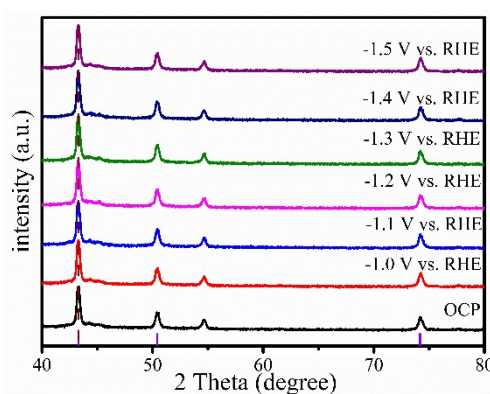


Fig. S3. Potential-resolved operando XRD patterns of the Cu.

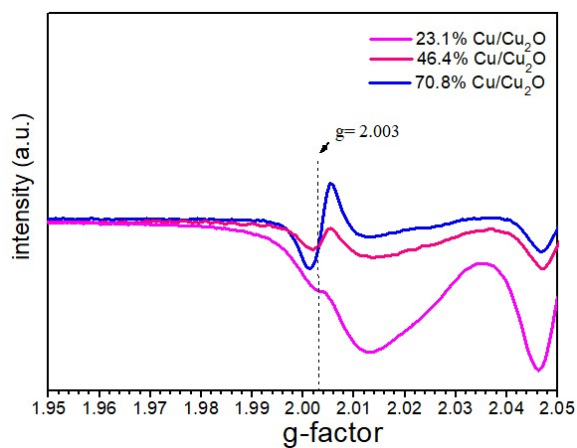


Fig. S4. EPR results for 23.1% Cu/Cu₂O, 46.4% Cu/Cu₂O and 70.8% Cu/Cu₂O.

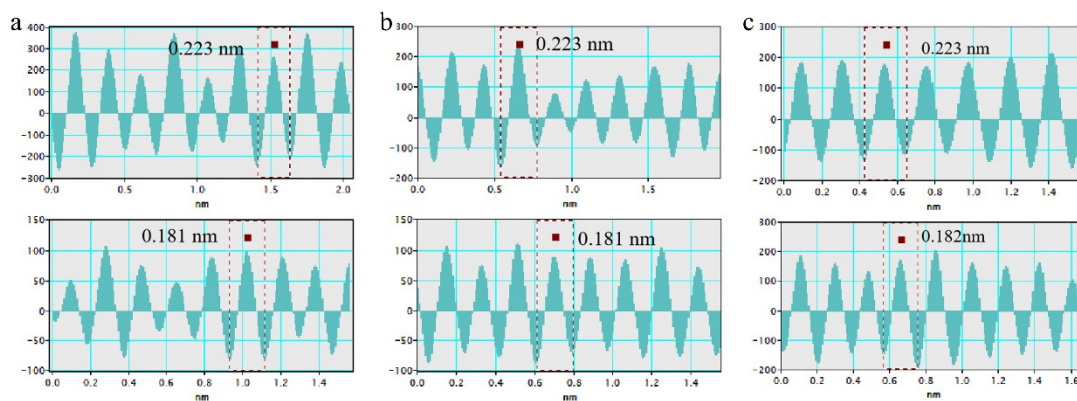


Fig. S5. Inverse FFT interplanar spacing profiles of 23.1% Cu/Cu₂O, 46.4% Cu/Cu₂O and 70.8% Cu/Cu₂O.

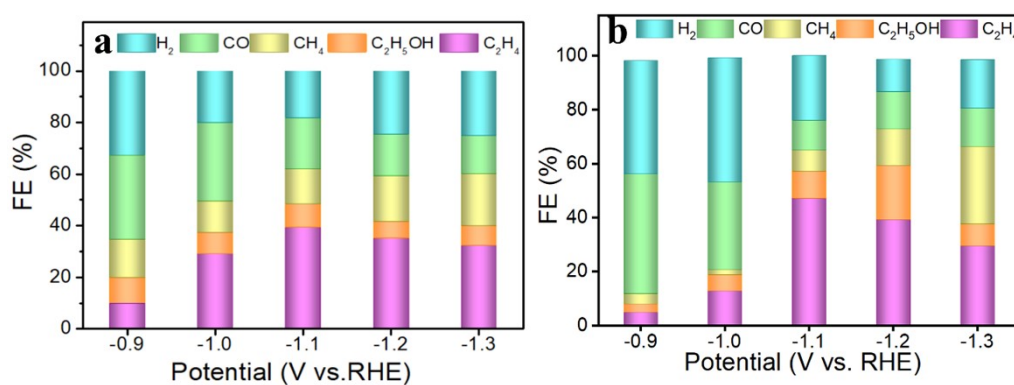


Fig. S6. Faradaic efficiencies for C₂H₄, CO, CH₄ and H₂ on (a) 23.1% Cu/Cu₂O and (b) 70.8% Cu/Cu₂O at different applied potentials, respectively.

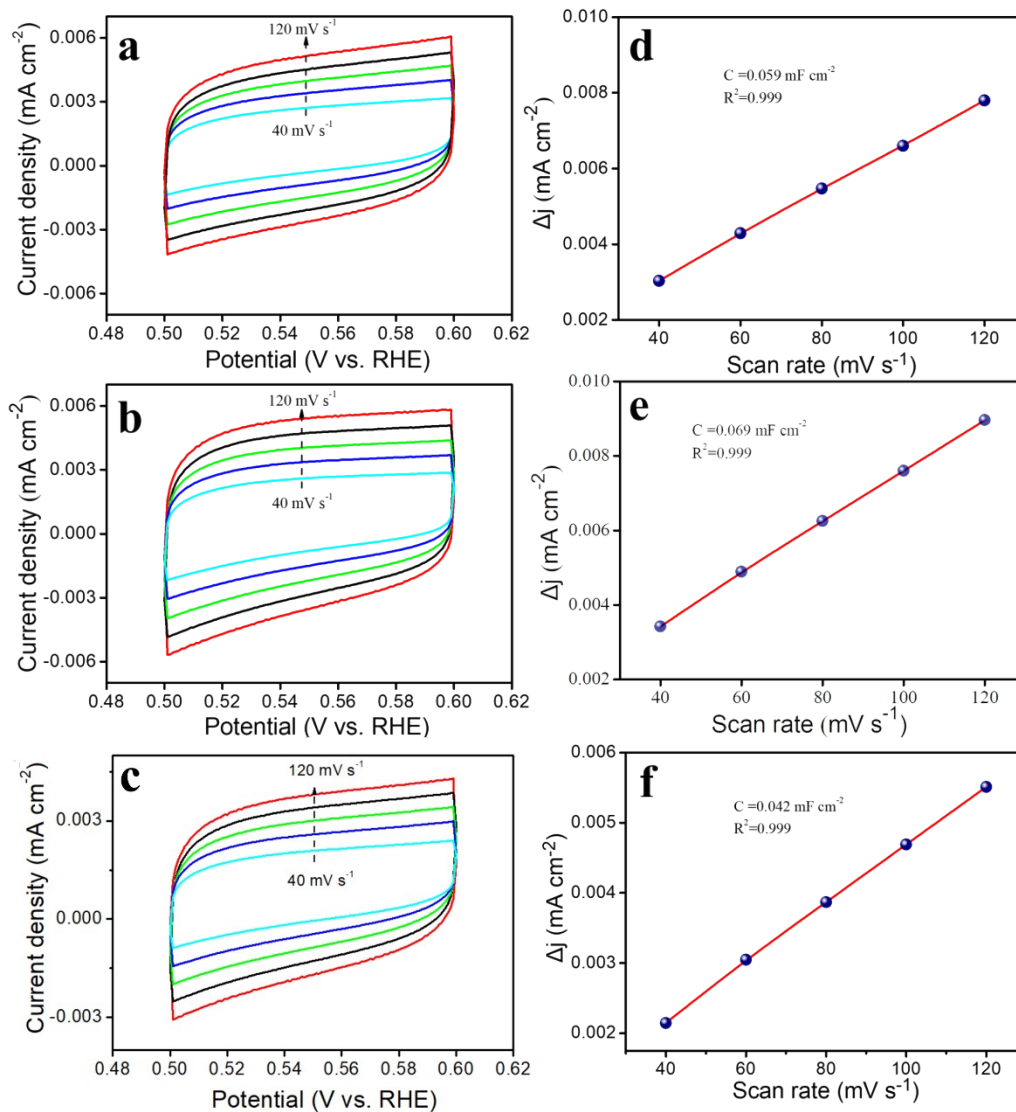


Fig. S7. ECSA measurement. (a-c) CVs with various scan rates between 0.49 - 0.59 V vs. RHE in CO₂-saturated 0.1 M KHCO₃ solution for determining CdI for (a) 23.1% Cu/Cu₂O, (b) 46.4% Cu/Cu₂O and (c) 70.8% Cu/Cu₂O, respectively; double layer capacitance of (d) 23.1% Cu/Cu₂O, (e) 46.4% Cu/Cu₂O and (f) 70.8% Cu/Cu₂O, respectively.

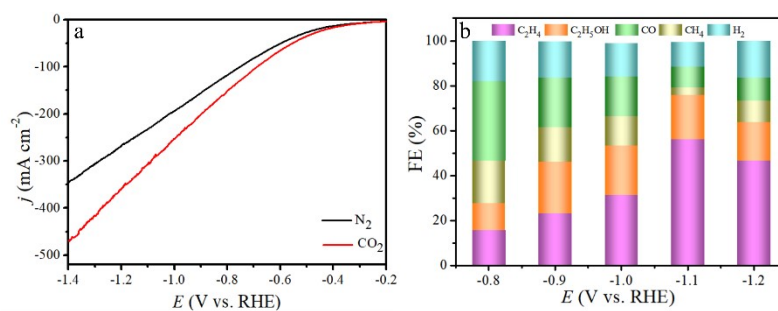


Fig. S8. Electrocatalytic CO₂RR performances of 46.4% Cu/Cu₂O in a flow-cell with 1 M KOH electrolyte. (a) LSV curves were measured in 1 M KOH solution saturated with N₂ or CO₂. (b) Current-dependent FEs of various reduction products

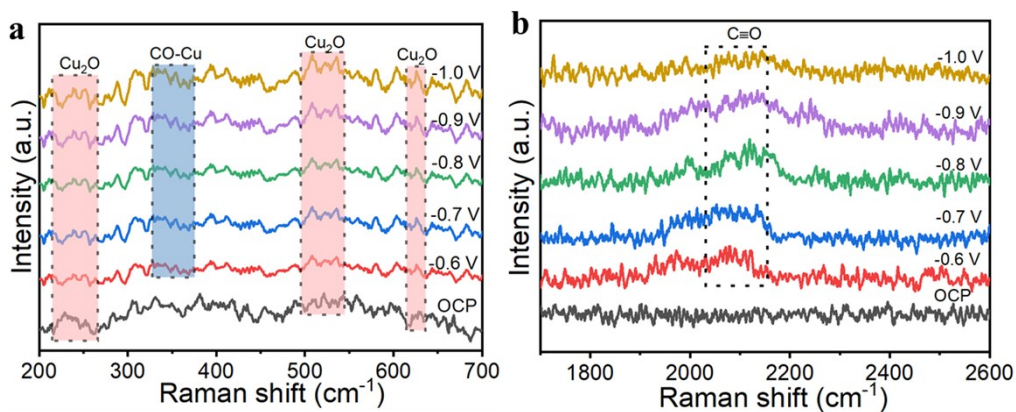


Fig. S9. In situ Raman spectra of CO₂RR over 46.4% Cu/Cu₂O as a function of the applied potentials.

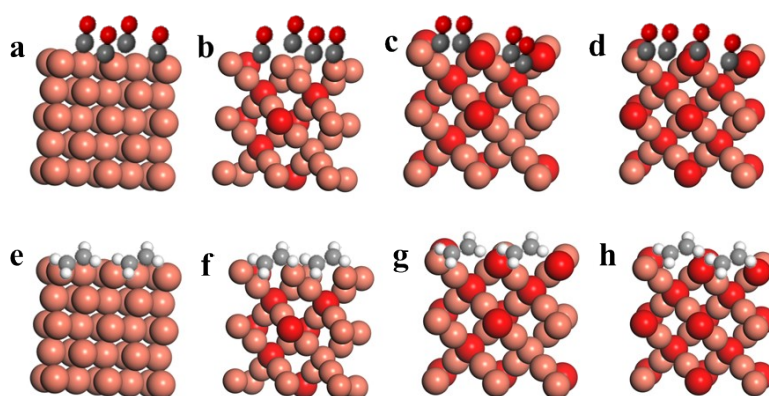


Fig. S10. The CO and C₂H₄ adsorption configurations on (a and e) Cu, (b and f) 23% Cu/Cu₂O, (c and g) 46% Cu/Cu₂O, and (d and h) 71% Cu/Cu₂O.

Table S1. Diffraction peak shifts and the corresponding lattice parameters and strain values observed during the *operando* XRD on Cu₂O nanocrystals at different potentials. Cu foil was tested on the same XRD instrument as a reference.

Cu precursor	CO ₂ RR potential (VRHE)	Cu(111)			Cu(200)		
		Average XRD peak position (2θ)	Lattice parameter (Å)	Strain(%)	Average XRD peak Position (2θ)	Lattice parameter (Å)	Strain(%)
Cu foil		43.388	3.6123	0	50.519	3.6133	0
Cu/Cu ₂ O	-1.1	43.342	3.6128	0.01	50.475	3.6161	0.07
	-1.2	43.287	3.6172	0.22	50.318	3.6236	0.29
	-1.3	43.232	3.6216	0.34	50.263	3.6274	0.39

Table S2. The content of Cu⁺ and Cu⁰ on Cu/Cu₂O samples obtained by XPS.

Catalysts	Copper species (wt %)		
	Cu ⁺	Cu ⁰	Cu ⁺ /Cu ⁰
23.1% Cu/Cu ₂ O	76.9	23.1	3.33
46.4% Cu/Cu ₂ O	53.6	46.4	1.16
70.8% Cu/Cu ₂ O	29.2	70.8	0.41

Table S3. The content of O_L, O_V and O_W on the surface of the different Cu/Cu₂O samples obtained by XPS.

Catalysts	Oxygen species (wt %)		
	O _L	O _V	O _W
23.1% Cu/Cu ₂ O	33.4	21.5	45.1
46.4% Cu/Cu ₂ O	29.9	54.6	15.4
70.8% Cu/Cu ₂ O	10.5	74.4	15.1

Table S4. Catalytic performances of Cu-based catalysts

Catalyst	Electrolyte	FE _(C₂H₄)	E vs. RHE	Ref.
CuO _x	0.5 M KHCO ₃	54%	-1.4V	1
Cu-Pd bimetallic	0.1 M KCl	45.2%	-1.2 V	2
Ag ₁ -Cu _{1.1}	0.1 M KHCO ₃	40%	-1.1 V	3
CuNi-2	0.5 M NaHCO ₃	24%	-0.97V	4
Cu@Ag Core-Shell	1M KOH	32.2%	-1.1 V	5
Cu@Cu NS-12	0.1M KHCO ₃	40.7%	-1.357V	6
Cu _y /CeO ₂	0.1 M KHCO ₃	42%	-1.3V	7
GB-Cu	1M KOH	38%	-1.2V	8
Cu _y -Cu ₂ O	0.1 M KHCO ₃	51%	-0.76V	9
Cu@nanosilica	0.1 M KHCO ₃	46%	-1.4V	10
CuO microboxes	0.1 M K ₂ SO ₄	49.6%	-1.05V	11
46.4% Cu/Cu ₂ O NCs	0.1 M KHCO ₃	52.5%	-1.1V	This work